LA-UR- 08-6751

Approved for public release; distribution is unlimited.

Title: Diameter-dependent electronic transport properties of Au-catalyst/Ge-nanowire Schottky diodes

Author(s): S.T. Picraux, LANL
Francois Swartzentruber, SNL
A. Alec Talin, SNL

Intended for: Physical Review Letters - Journal

Los Alamos
NATIONAL LABORATORY
EST. 1943

Los Alamos National Laboratory, an affirmative action/equal opportunity employer, is operated by the Los Alamos National Security, LLC for the National Nuclear Security Administration of the U.S. Department of Energy under contract DE-AC52-06NA25396. By acceptance of this article, the publisher recognizes that the U.S. Government retains a nonexclusive, royalty-free license to publish or reproduce the published form of this contribution, or to allow others to do so, for U.S. Government purposes. Los Alamos National Laboratory requests that the publisher identify this article as work performed under the auspices of the U.S. Department of Energy. Los Alamos National Laboratory strongly supports academic freedom and a researcher's right to publish; as an institution, however, the Laboratory does not endorse the viewpoint of a publication or guarantee its technical correctness.

Form 836 (7/06)

Diameter-dependent electronic transport properties of Au-catalyst/Ge-nanowire Schottky diodes

François Léonard[1*], A. Alec Talin[1], B. S. Swartzentruber[2], and S. T. Picraux[3]

[1] *Sandia National Laboratories, Livermore, California 94551*

[2] *Sandia National Laboratories, Albuquerque, New Mexico 87185*

[3] *Los Alamos National Laboratory, Los Alamos, New Mexico, 87545*

(Dated: October 7, 2008)

We present electronic transport measurements in individual Au-catalyst/Ge-nanowire interfaces demonstrating the presence of a Schottky barrier. Surprisingly, the small-bias conductance density increases with decreasing diameter. Theoretical calculations suggest that this effect arises because electron-hole recombination in the depletion region is the dominant charge transport mechanism, with a diameter dependence of both the depletion width and the electron-hole recombination time. The recombination time is dominated by surface contributions and is found to depend linearly on the nanowire diameter.

Semiconductor nanowires show promise as active elements in electronic [1, 2], optoelectronic [3, 4], and sensing [5] devices. Often, metal-catalyzed chemical vapor deposition is used to grow the nanowires, with Au the most frequent catalyst metal. Typically, a small hemispherical Au particle remains attached on the tip of the nanowires after the growth is ceased [6]. To date, the electrical nature of the Au-catalyst/nanowire junction remains largely unknown. Yet, there are several scientific and technological reasons to explore the electronic transport characteristics of such contacts. For example, catalyst/nanowire junctions offer a unique opportunity to examine how nanoscale dimensions affect contact properties; and rectifying contacts to free-standing, vertically oriented nanowires could prove useful in a number of applications such as Schottky detectors and mixers, where the very low capacitance associated with the nanoscale diameter could lead to higher operating frequency, and the bottom-up assembly could reduce fabrication costs.

Here, we use a microprobe retrofitted inside of a scanning electron microscope (SEM) to examine the charge injection at Au-catalyst/Ge-nanowire interfaces and subsequent transport in the Ge nanowire. Our measurements indicate that this interface is rectifying with a large Schottky barrier. Remarkably, the current density *increases* with decreasing nanowire diameter, in contrast to common expectations. By modeling the nanowire electrostatics, we show that this arises because the current is dominated by electron-hole recombination in the depletion region, a contribution which is usually negligible in bulk junctions, but is strongly enhanced in nanowires due to the increased importance of surface recombination. Combining the modeling results with the experimental data, we find that the recombination time decreases as the nanowire diameter is decreased; a simple theory including bulk and surface recombination explains this result. The surface recombination velocity is found to be $\sim 10^5 cm/s$, comparable to that of planar Ge surfaces, and in agreement with recent ultrafast time-resolved optical measurements in nanowires [8].

The growth of Ge nanowires was performed in a cold wall chemical vapor deposition system by the vapor-liquid-solid technique[9] at a temperature ~375 °C and total pressure of 1.5 Torr. A 30% GeH_4 precursor in H_2 along with 100 ppm PH_3 in H_2 as the source of the n-type dopant was used with the gas flows set for a 1.2×10^{-3} P to Ge atom ratio. Au colloids were used as the catalytic growth seeds on heavily doped (0.06Ω-cm) n-type Ge (111) substrates with acidified deposition of the colloids immediately prior to introduction into the growth chamber to achieve predominately vertical nanowires growth.

The electrical measurements were carried out by contacting individual vertically-oriented nanowires directly on the growth substrate using a piezomotor controlled, Au-coated W probe retrofitted inside of a JEOL SEM and connected to an Agilent semiconductor parameter analyzer. A SEM image of the probe near as-grown Ge nanowires is shown in the inset of Fig. 1a. Most nanowires are ~100 nm in height and have diameters from 20 nm to 150 nm. Virtually all of the nanowires are capped with the hemispherical Au catalyst nanoparticle.

The current-voltage characteristics of a nanowire of 54 nm diameter is shown in the main panel of Fig. 1a. The behavior is clearly rectifying, as observed in almost all of the nanowires. This rectifying behavior is consistent with that observed at bulk Au/Ge interfaces [10], where a large Schottky barrier of 0.59 eV is present, and is essentially independent of the type of metal because Ge is one of the semiconductors with the strongest Fermi level pinning. Our observations are also consistent with atom-probe tomography measurements [7] which indicated an abrupt interface between the Au catalyst nanoparticle and the Ge nanowires. It is tempting to analyze the rectifying behavior using conventional thermionic emission theory to extract the Schottky barrier. However, a surprising observation does not fit into existing theories of

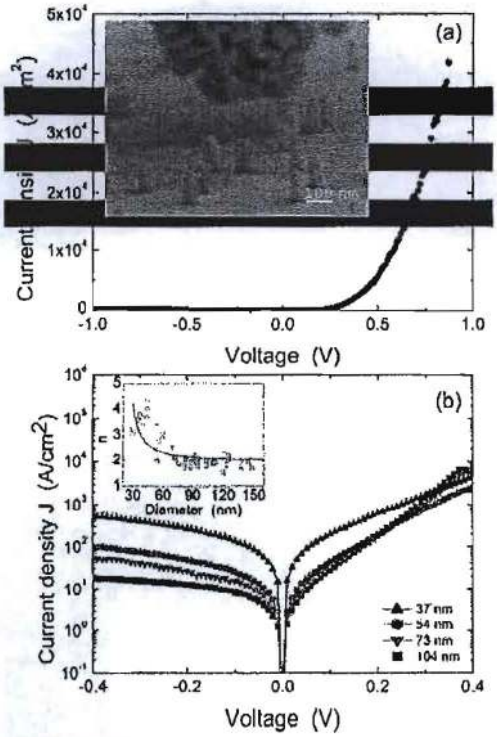

FIG. 1: Panel(a) shows current-voltage characteristics for a Ge nanowire of 54 nm diameter. The inset is a SEM image of the Au-coated W tip and several Ge nanowires. Panel (b) shows current-voltage curves on a log scale, for four nanowires of different diameters. The inset shows the ideality factor measured at forward bias as a function of nanowire diameter.

electronic transport through Schottky barriers.

The observation, as shown in Fig. 1b, is that the small-bias conductance density and reverse-bias current density are found to depend strongly on the nanowire diameter, and in fact, *increase* with decreasing diameter. This is contrary to most models of transport in nanowires, where the increased importance of surface scattering *reduces* the small-bias conductance when the diameter is decreased. In addition, the phenomenon cannot be explained based on a reduction of the effective Schottky barrier height due to increased tunneling at smaller dimensions because the depletion width actually increases with decreasing diameter, as we will show below. To understand the experimental observations, and why the current-voltage characteristics of Fig. 1b cannot be analyzed using thermionic emission theory, we first consider the total current density in a Schottky diode; this can be written as $J = J_{th} + J_{rn} + J_{rd}$, where J_{th} is the thermionic current density, J_{rn} is the electron-hole recombination current density in the neutral region, and J_{rd} is the electron-hole recombination current density in the depletion region. The first contribution is of the form [11] $J_{th} = A^* T^2 \exp(-\phi_b/kT)\left[\exp(eV/kT) - 1\right]$ with A^* the Richardson constant, ϕ_b the Schottky barrier height, V the applied voltage, k Boltzmann's constant, and T temperature. In most diodes, this term dominates the behavior. In the present case however, this contribution is negligible because of the large Schottky barrier of 0.59 eV; indeed, the small-bias conductance due to this term, $dJ/dV = \left(eA^*T^2/kT\right)\exp(-\phi_b/kT) \sim 10^{-2} A/cm^2V$, is much smaller than that measured experimentally $\left(\sim 1 - 20\ A/cm^2V\right)$. Similarly, the second term [11], $J_{rn} = \left(n_i^2/N_d\right)\left(ekT\mu/\tau\right)^{1/2}\left[\exp(eV/kT) - 1\right]$ with μ the carrier mobility, n_i the intrinsic carrier concentration, N_d the dopant concentration, and τ the electron-hole recombination time, gives a negligible small-bias conductance even with very low values of the recombination time. Thus, we are left with the contribution [11]

$$J_{rd} = J_0\left[\exp\left(\frac{eV}{2kT}\right) - 1\right]. \qquad (1)$$

By analyzing the $J - V$ curves of the nanowires with the functional form $J \propto \left[\exp(eV/nkT) - 1\right]$, we extract an ideality factor $n = 2$ for the larger nanowires as shown in the inset of Fig. 1b, in agreement with Eq. (1). This suggests that electron-hole recombination in the depletion region is the dominant transport mechanism in these nanoscale contacts. (The reason for the larger values of n at smaller diameters will be discussed below.)

To further explore the role of electron-hole recombination, we performed calculations of the small bias conductance of Ge nanowires. The small-bias conductance density is written as[11]

$$\left.\frac{dJ_{rd}}{dV}\right|_{V=0} = \frac{e}{2kT}\frac{1}{\tau(d)}\int_0^L \frac{n_i^2}{n(z) + p(z) + 2n_i}dz \qquad (2)$$

where $n(z)$ and $p(z)$ are the electron and hole concentration at position z along the nanowire of length L. In anticipation of the results below, we have written the recombination time as being diameter dependent. The term inside of the integral corresponds to the local recombination rate, assumed to be independent of the radial coordinate, an assumption that is supported by our three-dimensional calculations that we now describe.

To obtain the carrier concentrations $n(z)$ and $p(z)$, we calculate self-consistently the charge and the electrostatic potential at zero bias, for the geometry of Fig. 2. There, a Ge nanowire of diameter d, length 100 nm, and dielectric constant ε is making contact to a bulk metal on one side and to the Ge substrate on the other side. The nanowire is n-doped with dopant concentration of $10^{18} cm^{-3}$, and is surrounded by vacuum. We solve Poisson's equation with the spatially varying charge on the nanowire and with appropriate boundary conditions: at the metal/nanowire interface, the strong Fermi level pinning fixes the electrostatic potential to give a Schottky barrier of 0.59 eV, while at the nanowire/substrate interface the potential gives charge neutrality for a doping of $10^{18} cm^{-3}$. Boundary conditions are also applied

at the nanowire surface to produce the electric field discontinuity due to the different dielectric constants of the nanowire and vacuum, and far away from the nanowire (1 micron in practice) the radial electric field vanishes. The local charge in the nanowire is calculated by integrating the bulk density of states for Ge (shifted by the local electrostatic potential) times the Fermi function. We also consider the fact that Ge surfaces contain a large density of surface states [12], a fact also true for Ge nanowires [1]. We thus include a density of surface states of 0.01 states/eV/atom at the surface of the Ge nanowire exposed to vacuum (our conclusions are unchanged even if we vary this surface state density by an order of magnitude). These surface states are modeled as a uniform density of electronic states in the Ge bandgap, with a neutrality level at midgap; they decay exponentially into the nanowire with a decay length of 0.3 nm.

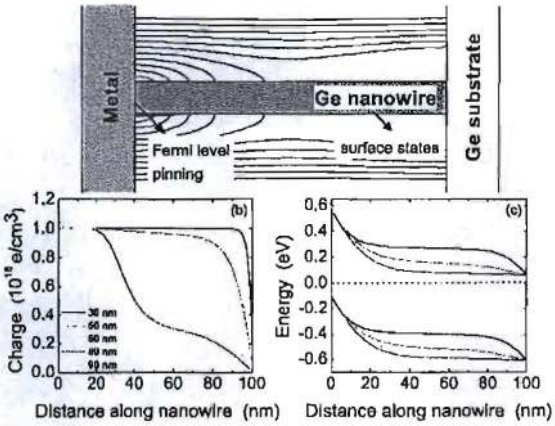

FIG. 2: (Color online) (a) Sketch of the system used for the numerical calculations, see text for details. The calculated electric field lines are shown for a nanowire of 30 nm diameter. (b) Calculated charge in the center of the nanowire as a function of distance along the nanowire. (c) Calculated band-bending. In (b) and (c) the curves from top to bottom correspond to nanowires diameters of 30, 50, 60, 80, and 90 nm.

Figure 2 shows the calculated self-consistent charge and band-bending for nanowires of different diameters. Near the metal/nanowire interface, the nanowire is of p^+ character due to the position of the Fermi level close to the valence band. A depletion region then extends over a length that increases strongly as the nanowire diameter is decreased. As a consequence, the total recombination current density in the depletion region increases with decreasing diameter. To see if this behavior is sufficient to explain our experimental data, we calculated the small bias conductance from Eq. (2) assuming a *fixed* recombination time chosen to reproduce the large diameter values. When compared with the experimental data in Fig. 3, the calculated small bias conductance with the diameter-independent recombination time (dashed line) provides some increase with decreasing diameter, but is insufficient to give the amount of measured current and to reproduce the strong diameter dependence observed experimentally. Thus, we conclude that the total recombination time must depend on the nanowire diameter. To extract it from our experimental data, we fit the calculated recombination current density to the experimental data in Fig. 3 using a diameter-dependent recombination time $\tau^{-1}(d) = \tau_{bulk}^{-1} + a/d$; this gives excellent agreement with the measurements as shown by the solid line in Fig. 3, with the value $a = 7.85 \times 10^5 cm/s$.

To understand the origin of the dependence of the recombination time on nanowire diameter, we consider an infinitely long nanowire of diameter d into which carriers of density n_0 are injected initially. These carriers relax by diffusing through the nanowire and recombining at the surface and in the bulk. Their time and spatial dependence satisfy the diffusion equation [13] $\partial_t n = D\nabla^2 n - n/\tau_{bulk}$ where D is the diffusion constant. At the nanowire surface, electron-hole recombination with surface recombination velocity s takes place, giving the boundary condition [13] $-D\left(\nabla n \cdot \hat{r}\right)_{r=d/2} = sn(d/2, t)$. The solution of these equations gives an exponential time decay of the carrier density, with the smallest time constant $\tau^{-1} = \tau_{bulk}^{-1} + \lambda(s, D, d)$ where λ satisfies

$$D\lambda J_1\left(\lambda\frac{d}{2}\right) = sJ_0\left(\lambda\frac{d}{2}\right) \tag{3}$$

with J_ν a Bessel function of order ν. For the case $s \ll D/d$ (which applies to our data), one can use the small argument behavior of the Bessel functions in Eq. (3) to obtain $\lambda = 4s/d$ and

$$\frac{1}{\tau} = \frac{1}{\tau_{bulk}} + \frac{4s}{d}. \tag{4}$$

Thus, the total recombination time is reduced by the presence of the surface term. Comparing with our fit to the experimental data in Fig. 3, we extract $s \approx 2 \times 10^5 cm/s$; this value is consistent with that recently measured on similar Ge nanowires using ultrafast time-resolved optical measurements [8]. (The theory predicts $\tau^{-1}(d) = \tau_{bulk}^{-1} + 3\pi D/d^2$ in the limit $s \gg D/d$, and such a function could be fitted to the data of Fig. 3. However, this leads to a value for D that is two orders of magnitude lower than typical values for Ge.)

The dominance of electron-hole recombination in this system also explains the large ideality factors measured at forward bias for the smaller nanowires. Because the recombination current is essentially an integration over the depletion region[11], $J_{rd} \sim W(V)\left[\exp\left(eV/2kT\right) - 1\right]$, where the bias dependence of W arises because the built-in potential is reduced to $V_{bi} - V$ at forward bias. In bulk diodes, this leads to a mild dependence $W_{bulk}(V) = \sqrt{2\varepsilon\left(V_{bi} - V\right)/eN_d}$, with little impact on the ideality factor. However, for a nanowire W depends exponentially on the applied voltage, as we now discuss.

To calculate the depletion width, we approximate the charge distributions in Fig. 2b as $\rho(r, z) =$

$-eN_d[1-\theta(r-d/2)]$ for $0 < z < W_{NW}$, where W_{NW} is the nanowire depletion width. The electrostatic potential *at the center* of the wire is then $V(z) = \int_0^{d/2}\int_0^{W_{NW}} G(r=0,z;r',z')\,r'dr'dz'$, where $G(r,z;r',z')$ is the electrostatic green's function with the boundary conditions that the derivative of the potential at the nanowire surface be discontinuous by the ratio of dielectric constants of the environment and nanowire; G also includes the contribution from image charges in the metal, and can be obtained using standard techniques. With the requirement that $V(z)$ at the edge of the depletion layer give the built-in voltage V_{bi} this allows us to obtain (in the limit $W_{NW}/d \gg 1$)

$$W_{NW} \approx d\exp\left(8\frac{\varepsilon_0}{\varepsilon}\frac{W_{bulk}^2}{d^2}\right). \quad (5)$$

This relationship is similar to that obtained for carbon nanotubes [14].

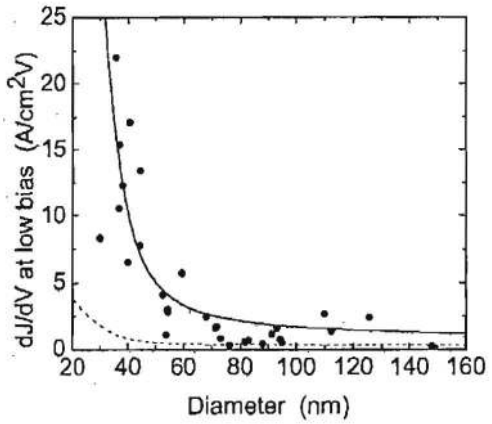

FIG. 3: Small-bias conductance density of the Au-nanoparticle/Ge-nanowire interface as a function of the nanowire diameter. The dashed (solid) line is calculated with a diameter-independent (-dependent) recombination time.

The exponential dependence of W_{NW} explains the large forward bias ideality factors shown in the inset of Fig. 1b. Indeed, we have $W_{NW}(V) \sim \exp(-16\varepsilon_0 V/eN_d)$ giving $J_{rd} \sim \exp\left(\frac{eV}{n_{eff}kT}\right)$ with

$$n_{eff} = 2\left(1-\frac{l^2}{d^2}\right)^{-1}. \quad (6)$$

Thus, the ideality factor increases as the nanowire diameter is reduced below the length scale $l = \sqrt{32kT\varepsilon_0/e^2N_d}$. This behavior can be tested by numerically fitting the data in the inset of Fig. 1b. As shown by the solid line, this provides a good description of the measured ideality factor with the value $l \approx 22nm$; this compares reasonably with the value of $7nm$ predicted by the expression for l. (We also note that at reverse bias, the depletion width should increase exponentially with voltage, explaining the lack of saturation observed in our measurements. But because W_{NW} increases so rapidly, it can quickly reach the finite length of the nanowire and start to deplete the substrate, leading to a more complicated dependence on voltage. However, it is clear from Fig. 1b that the reverse bias current density increases more strongly as the diameter is reduced.)

To summarize, the unusual diameter-dependent electronic transport in the Au-catalyst/Ge-nanowire system originates from a combination of several effects: the strong Fermi level pinning at the Au/Ge interface leads to a large Schottky barrier and a negligible contribution of thermionic emission to the total current. As a consequence, electron-hole recombination in the depletion region dominates the current. This leads to an increase of the zero-bias conductance density as the nanowire diameter is reduced because the depletion width increases with decreasing diameter and the recombination time decreases due to the increased importance of the surface. The strong dependence of the depletion width on applied voltage leads to very large ideality factors at forward bias. More generally, our results suggest that the electronic transport properties of nanoscale contacts can differ significantly from those of their bulk counterparts.

Work performed in part at the U.S. Department of Energy, Center for Integrated Nanotechnologies, at Los Alamos National Laboratory and Sandia National Laboratories.

*email:fleonar@sandia.gov

REFERENCES

[1] D. Wang *et al.*, J. Am. Chem. Soc. **125**, 11602 (2005).
[2] J. Goldberger *et al.*, Nano Lett. **6**, 973 (2006).
[3] X. Duan, *et al.*, Nature **409**, 66 (2001).
[4] H. Pettersson *et al.*, Nano Lett. **6**, 229 (2006).
[5] G. Zheng *et al.*, Nat. Biotechnol. **23**, 1294 (2005).
[6] S. Kodambaka *et al.*, Phys. Rev. Lett. **96** 096105 (2006).
[7] D.E. Perea *et al.*, J. Solid State Chem. **181**, 1645 (2008).
[8] R.P. Prasankumar *et al.*, Nano Lett. **8**, 1619 (2008).
[9] J.W. Dailey *et al.*, J. Appl. Phys. **96**, 7556 (2004).
[10] T. Nishimura, K. Kita, and A. Toriumi, Appl. Phys. lett. **91**, 123123 (2007).
[11] S. M. Sze, Physics of semiconductor devices, (Wiley, New York 1980).
[12] M. Elices and F. Ynduráin, J. Phys. C: Solid State Phys. **5**, L146 (1972).
[13] J.P. McKelvey and R.L. Longini, J. Appl. Phys. **25**, 634 (1954).
[14] F. Léonard and J. Tersoff, Phys. Rev. Lett. **83**, 5174 (1999).